Progress In Electromagnetics Research M, Vol. 29, 109–119, 2013

ISOLATED OPEN-RING DEFECTED GROUND STRUCTURE TO REDUCE MUTUAL COUPLING BETWEEN CIRCULAR MICROSTRIPS: CHARACTERIZATION AND EXPERIMENTAL VERIFICATION

Sujoy Biswas[1, *] and Debatosh Guha[2]

[1]Institute of Technology and Marine Engineering, Jhinga, Diamond Harbour Road, Amira, South 24 Paraganas, WB 743368, India

[2]Institute of Radio Physics and Electronics, University of Calcutta, 92, Acharya Prafulla Chandra Road, Kolkata 700009, India

Abstract—A recently developed technique to design and model isolated Defected Ground Structure (DGS) has been examined to control coupling between two adjacent elements in a microstrip array. This is the only technique that can handle isolated DGS and in here, this is explored for the first time in microstrip antenna domain. An X-band design is presented. A set of prototypes are used to obtain measured data which are employed to verify the technique experimentally for microstrip array.

1. INTRODUCTION

Defected Ground Structure (DGS) and its applications have been discussed in a recent book [1]. A DGS is conventionally characterized by its stop-band characteristics when it is placed beneath a microstrip line and this has been popular for printed circuit applications. Application of DGS to improve the radiation properties of printed antennas has been a new topic initiated by this research group in 2005 [2]. The possibility of suppressing mutual coupling using DGS in between two adjacent microstrip array elements was proposed in [3, 4]. This idea has been extended to specific application like reducing scan blindness in microstrip arrays [5, 6]. DGS was also explored to reduce mutual coupling between dielectric resonator antennas [7]. In recent years, different researchers have studied different DGS geometries

Received 14 December 2012, Accepted 12 February 2013, Scheduled 14 February 2013

* Corresponding author: Sujoy Biswas (s_rpe@yahoo.co.in).

and configurations to reduce mutual coupling between microstrip elements [8–11].

For mitigating mutual coupling, the DGS is placed in between the radiating elements and is fully isolated from the antenna structure. But no standard technique to characterize and design such isolated DGS was known until [12]. Very recently, present authors have proposed a realistic solution [12]. This has been tested in dielectric resonator antenna (DRA) array. In this paper, we have examined this recently developed technique [12] in microstrip array environment. We have targeted to use open-ring DGS as in [12] for a pair of circular patches operating in X-band. Schematic diagram is shown in Fig. 1. We have designed and characterized the DGS, and have examined its suitability in controlling mutual coupling in planar microstrip two element array experimentally. Like [12], identical suppression by about 5 dB has been demonstrated.

2. DESIGN AND CHARACTERIZATION

Two E-plane coupled circular microstrips, separated by a distance of $\lambda_0/2$, is shown in Fig. 1. This also depicts an open-ring DGS as applied in [12], placed in between the two patches. Open-ring is chosen for a couple of reasons. Firstly to maintain symmetry with the patch geometry and secondly to compare with [12]. This open-ring geometry is derived from a full ring DGS by truncating it at a distance of t_r from its outer boundary as indicated in Fig. 1(b). The ring is characterized by the parameters like: outer radius r_0, inner radius r_i, ring width s, and average ring radius r_m $(= r_i + 0.5s)$. The design procedure of the open-ring DGS is described below.

In here, the radius a_r of the circular patch is determined using the formulations derived in [13] and this should operate around 10 GHz. The open-ring is concentric with one of the circular patches. To place the DGS at the midpoint between two circular patches, mean radius r_m of the ring is determined as $r_m = a_r + 0.5g = 7.5$ mm ($a_r = 5$ mm at 10 GHz for a substrate of thickness $t_{sub} = 1.575$ mm, dielectric constant $\varepsilon_{r,sub} = 2.3$ and $g = 5$ mm). Out of rest two parameters s and t_r, freedom in choosing s is limited depending upon the space available between the two patch antennas. For the present study, s is chosen as 1 mm. The DGS needs to be characterized to determine the truncation t_r which creates a stop-band around the resonant frequency of the patch, i.e., around 10 GHz. We have employed our technique proposed in [12] to characterize this isolated DGS.

In this technique, the defect is placed midway in a microstrip line-gap as shown in Fig. 2. The gap dimension 'g' is equal to edge-to-edge

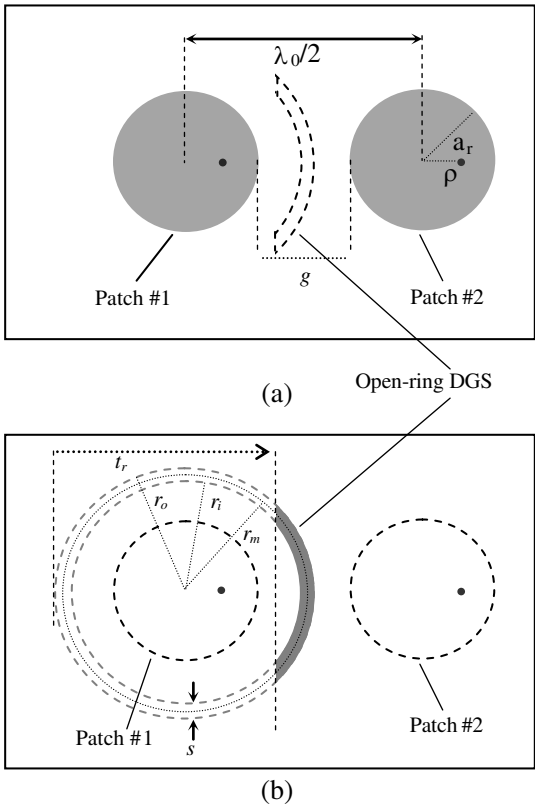

Figure 1. Two coax-fed E-plane coupled circular microstrip patch antennas with a open-ring DGS. (a) Top view. (b) Bottom view. Parameters: $t_{sub} = 1.575\,\text{mm}$, $\varepsilon_{r,sub} = 2.3$, $s = r_o - r_i = 1\,\text{mm}$, $r_0 = 8\,\text{mm}$, $r_i = 7\,\text{mm}$, $t_r = 12\,\text{mm}$, $a_r = 5\,\text{mm}$, $g = 5\,\text{mm}$, $\rho = 1.8\,\text{mm}$.

separation between two microstrip patches. Hence the defect is isolated and can interact only with the electromagnetic energy propagating through the dielectric medium across the gap g.

A DGS is considered as a resonant trap. The resonance property is determined by the defect dimensions r_m, s, and t_r. The effect of varying t_r (with $r_m = 7.5\,\text{mm}$ and $s = 1\,\text{mm}$) on the transmission characteristics of the line discontinuity (Fig. 2) is examined in Fig. 3. Simulated data are obtained using [14]. In absence of any defect, S_{21} increases monotonically with frequency. As soon as the DGS is incorporated in line-gap, propagation of electromagnetic (EM) fields is perturbed showing anomalous dispersion around DGS-resonance. This

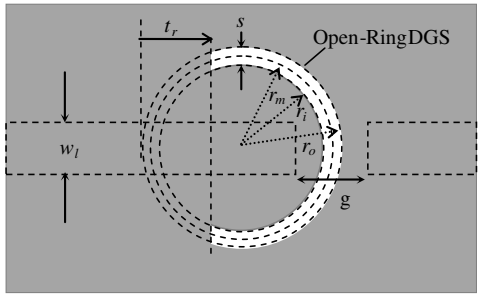

Figure 2. Open-ring DGS placed in between gap discontinuity in a 50 Ω microstrip line. Parameters: $w_l = 4.9\,\text{mm}$, $\varepsilon_{r,sub} = 2.3$, $t_{sub} = 1.575\,\text{mm}$.

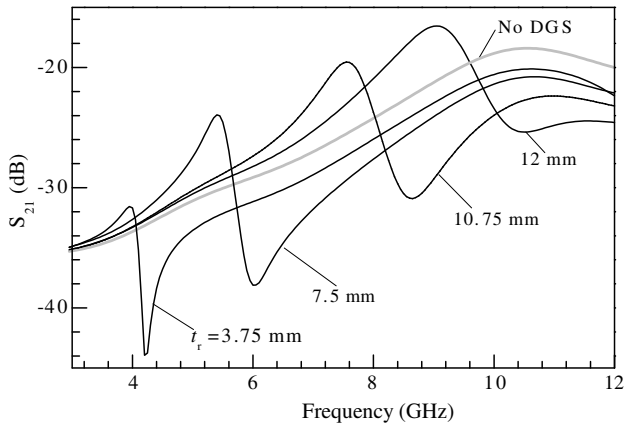

Figure 3. Simulated S_{21} of a line-gap discontinuity in a 50 Ω microstrip line with and without DGS. Parameters: $g = 5\,\text{mm}$, $s = 1\,\text{mm}$, $r_m = 7.5\,\text{mm}$. Substrate thickness $t_{sub} = 1.575\,\text{mm}$, relative permittivity of the substrate $\varepsilon_{r,sub} = 2.3$.

is evident from the S_{21} curves in Fig. 3 for varying t_r values. S_{21} minima indicate resonances in DGS as a function of parameter t_r. If the same DGS is integrated beneath the microstrip line, this would result in completely a different type of S_{21} characteristics as shown in Fig. 4. It is interesting to note that, the S_{21} plots in Fig. 4 reveal resonances identical to those obtained in Fig. 3, but in predicting relative isolations, they differ significantly. Fig. 3, obtained by our proposed technique [12], predicts around 5–6 dB isolation in the stop-band region. But the earlier approach, shown in Fig. 4, indicates its value of about 15–20 dB. Reliability of the proposed approach has been verified in Section 3. It is also observed from Fig. 3 that by varying t_r,

one can tune the DGS over a wide range of frequency without changing r_m or s value. For X-band design, $t_r = 12\,\text{mm}$ shows resonance occurring around 10 GHz along with relative isolation by about 6 dB.

An equivalent circuit model for the DGS placed in a gap-discontinuity of a microstrip line has also been developed for understanding the behavior. Since a DGS traps energy over a certain band of frequencies around resonance, it is modeled using a parallel LCR circuit [15, 16], as shown in Fig. 5(a). Equivalent circuit parameters can be calculated as [15].

$$C = \frac{\omega_c}{Z_0 g_1}\left(\frac{1}{\omega_0^2 - \omega_c^2}\right) \tag{1}$$

$$L = \frac{1}{4\pi^2 f_0^2 C} \tag{2}$$

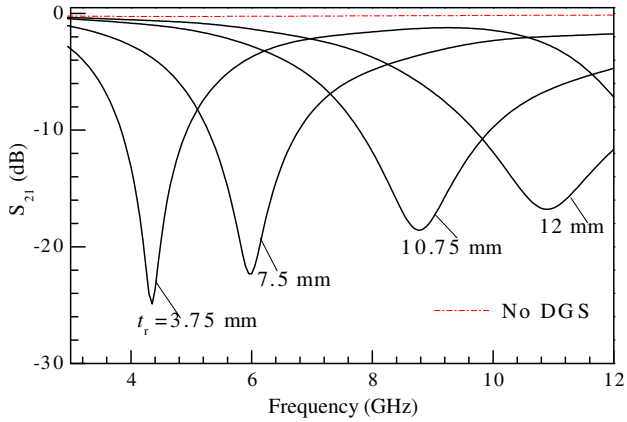

Figure 4. Simulated S_{21} characteristics of a 50 Ω continuous microstrip line integrated with the DGS. Parameters as in Fig. 3 with $g = 0$.

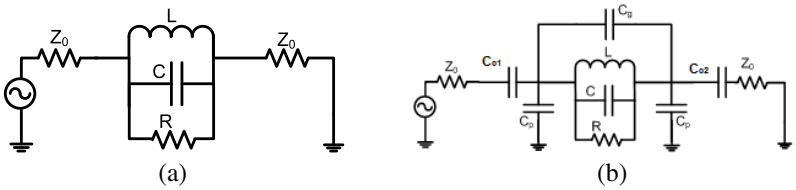

Figure 5. (a) Conventional parallel LCR equivalent circuit [15] of a DGS. (b) Equivalent LCR circuit of the DGS and the gap discontinuity in the 50 Ω microstrip line.

$$R = \frac{2Z_0}{\sqrt{\frac{1}{|S_{11}(\omega)|^2} - \left(2Z_0\left(\omega C - \frac{1}{\omega L}\right)\right)^2} - 1} \tag{3}$$

where, Z_0 is the characteristic impedance of the line, which is usually chosen as $50\,\Omega$. Other two parameters, i.e., ω_c and ω_0 are cut-off and resonant frequencies, respectively, and g_1 is the Butterworth low pass prototype filter element [17]. These are extracted from simulated S_{21} characteristics in Fig. 4.

Now, the DGS placed between a line-gap is modeled as shown in Fig. 5(b). Like in Fig. 5(a), parallel LCR represents the defect; equivalent components are determined using Eqs. (1)–(3). The microstrip line gap discontinuity is modeled using capacitances C_p and C_g [18]. Capacitance C_p is used to model the fringing fields near gap edges. Capacitance C_g across the line gap appears in parallel with the defect. Coupling capacitances C_{c1} and C_{c2} play a significant role in representing capacitive coupling between the line discontinuity and the defect. Open ring DGS ($t_r = 10.75\,\text{mm}$, $r_m = 7.5\,\text{mm}$, and $s = 1\,\text{mm}$) is used to verify the proposed circuit model. Calculated parameters are: $L = 1.27\,\text{nH}$, $C = 0.26\,\text{pF}$, and $R = 600\,\Omega$. The capacitances C_p and C_g across of the gap discontinuity are calculated using formulations in [18]. These capacitances along with the coupling capacitances C_{c1} and C_{c2} are optimized using circuit simulation tool [19]. Basis of the optimization is to match the circuit response of S_{21} with that using EM simulation [14] used for our study. The optimized values are: $C_p = 0.035\,\text{pF}$, $C_g = 0.02\,\text{pF}$, $C_{c1} = 0.012\,\text{pF}$ and $C_{c2} = 0.012\,\text{pF}$. Proposed model of DGS with line-gap is verified for open ring DGS in Fig. 6. Simulated S_{21} is compared with that obtained using equivalent circuit model and they show excellent mutual agreement. Measured S_{21} plot is added to confirm the verification experimentally.

3. EXPERIMENTS AND VERIFICATION

The design data, obtained in Section 2, have been examined and experimentally verified. The fabricated prototype is shown in Fig. 7. A similar prototype with normal ground plane is also fabricated and measured for comparison. Agilent's 8363B network analyzer is used for the measurement. Measured S_{21} are compared with the simulated data as shown in Fig. 8(a) and close agreement is revealed. Fig. 8(b) shows measured S_{11} and S_{22} responses. About 5 dB reduction in mutual coupling is revealed near 10.4 GHz. This value closely corroborates the predicted one shown in Fig. 3. Conventional approach indicated in Fig. 4 greatly differs from the reality.

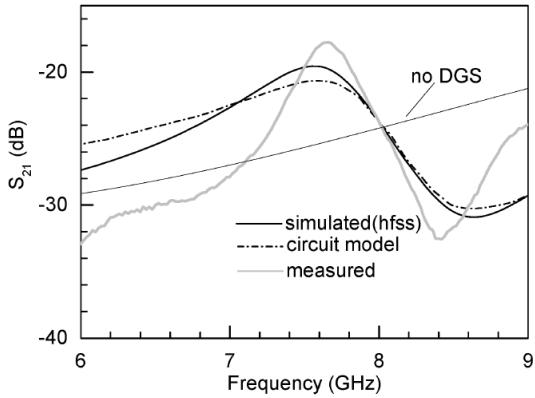

Figure 6. Comparison of simulated, measured and theoretical (circuit model) S_{21} versus frequency for open ring DGS. $t_r = 10.75\,\text{mm}$ and other parameters as in Fig. 3.

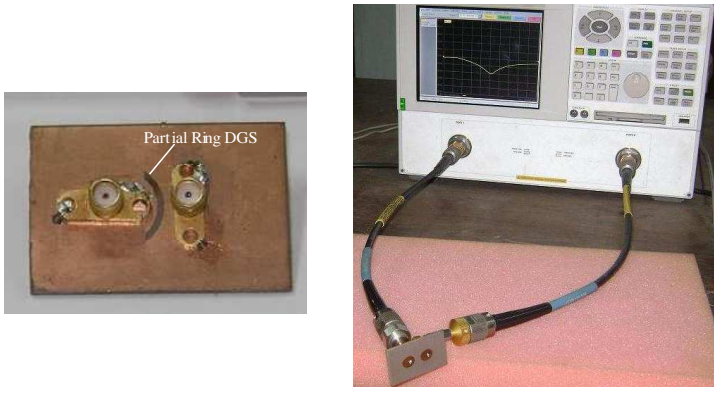

(a) (b)

Figure 7. Photograph of the Prototype. (a) Viewed from back-side. (b) Frontside view during measurement.

There is another important aspect to be discussed here. S_{21} characteristics shown in Fig. 3 are not repeated in Fig. 8(a). The reason is simple. Fig. 3 deals with the transmission of EM waves through a band-stop filter around the DGS-resonance; but in Fig. 8(a), the transmission (i.e., mutual coupling) takes place over a narrow band around the patch-resonance. Therefore, primarily it is like a band-pass operation. Now if a DGS having identical resonant frequency is added, the mutual coupling is suppressed. Therefore, explicit band-stop characteristics are not revealed and S_{21} in Fig. 8(a) does not

follow the same nature as in Fig. 3. The electrical phenomenon can be pictorially demonstrated as in Fig. 9. The ground plane current at resonance is quite indicative in the presence as well as absence of a defect. Considerable sharing of fields between adjacent elements is very prominent in the absence of the DGS. Presence of DGS greatly reduces that field.

The DGS suppresses mutual coupling and at the same time influences the radiation properties to some extent. An idea is obtained

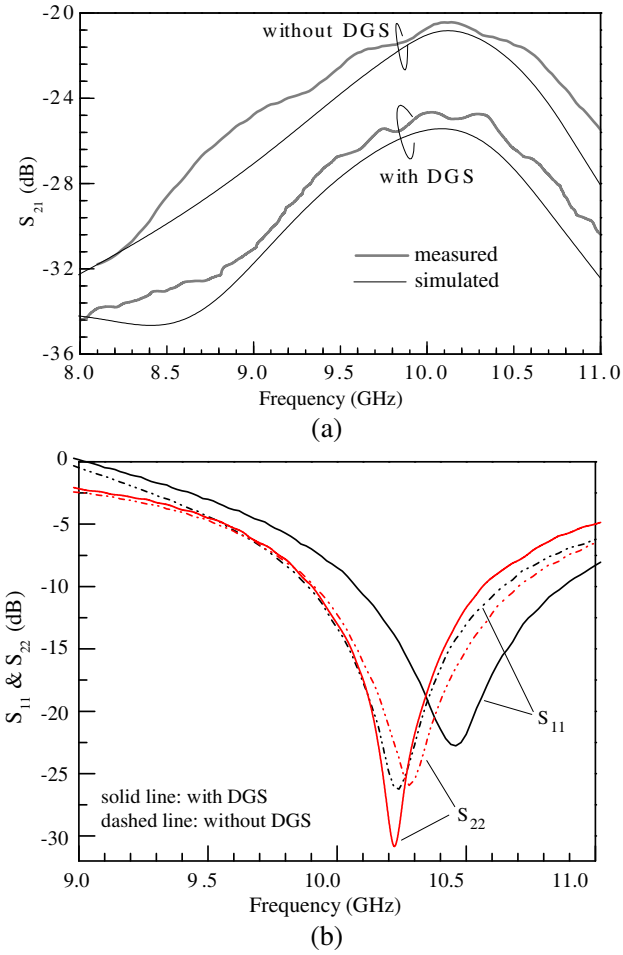

Figure 8. Measured data compared with simulated S-parameters for the prototype in Fig. 7. (a) S_{21} versus frequency. (b) S_{11} and S_{22} versus frequency. Parameters as in Fig. 1.

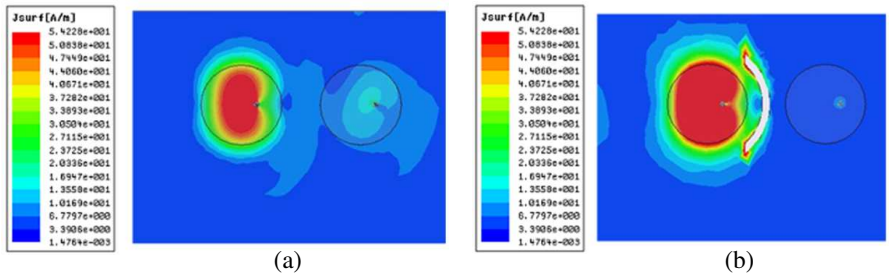

Figure 9. Surface current on the ground plane. (a) Conventional ground plane. (b) Ground plane with DGS. Parameters as in Fig. 1.

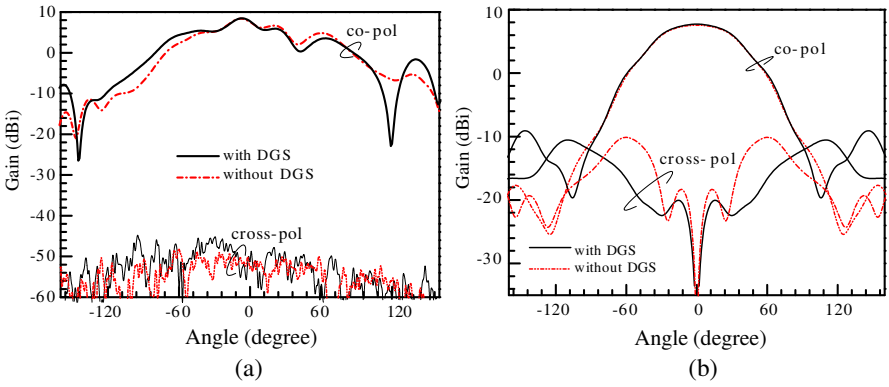

Figure 10. Simulated radiation patterns of the two element microstrip array. (a) E-plane, (b) H-plane. Parameters as in Fig. 1.

in Fig. 10. In either principal plane, the co-polarized patterns with and without DGS are found to be almost identical over $\pm 100°$. Beyond that, some degree of back radiation is apparent. This back radiation can be minimized over 50% by placing a secondary ground plane [3]. The peak gain is about 8dBi with normal ground plane and no appreciable change in gain is observed with DGS. It is interesting to note that the cross-polarized radiation in H-plane is considerably reduced up to $\pm 70°$. No change in the E-plane cross polarized radiation is observed.

4. CONCLUSION

An isolated DGS now can be accurately characterized and safely implemented in practical design of microstrip antenna array. Open-ring DGS is tested here. Other possible geometries may be explored

for improved performance, especially to improve the suppression of coupling and minimizing back radiation.

REFERENCES

1. Guha, D. and Y. M. M. Antar, *Microstrip and Printed Antennas: New Trends, Techniques and Applications*, Ch. 12, Wiley, UK, 2011.
2. Guha, D., M. Biswas, and Y. M. M. Antar, "Microstrip patch antenna with defected ground structure for cross polarization suppression," *IEEE Antennas Wireless Propagation Lett.*, Vol. 4, 455–458, 2005.
3. Guha, D., S. Biswas, M. Biswas, J. Y. Siddiqui, and Y. M. M. Antar, "Concentric ring-shaped defected ground structures for microstrip applications," *IEEE Antennas Wireless Propagation Lett.*, Vol. 5, 402–405, 2006.
4. Salehi, M., A. Motevasselian, A. Tavakoli, and T. Heidari, "Mutual coupling reduction of microstrip antennas using defected ground structure," *10th IEEE International Conference on Communication Systems*, 1–5, 2006.
5. Moghadas, H., A. Tavakoli, and M. Salehi, "Elimination of scan blindness in microstrip scanning array antennas using defected ground structure," *Int. J. Electron. Commun. (AEÜ)*, 155–158, 2008.
6. Hou, D.-B., et al., "Elimination of scan blindness with compact defected ground structures in microstrip phased array," *IET Microwave Antennas Propag.*, Vol. 3, No. 2, 269–275, 2009.
7. Guha, D., S. Biswas, T. Joseph, and M. T. Sebastian, "Defected ground structure to reduce mutual coupling between cylindrical dielectric resonator antennas," *Electronic Lett.*, Vol. 44, 836–837, 2005.
8. Mahmoudian, A. and J. Rashed-Mohassel, "Reduction of EMI and mutual coupling in array antennas by using DGS and AMC structures," *PIERS Online*, Vol. 4, No. 1, 36–40, 2008.
9. Zulkifli, F. Y., E. T. Rahardjo, and D. Hartanto, "Mutual coupling reduction using dumbbell defected ground structure for multiband microstrip antenna array," *Progress In Electromagnetics Research Letters*, Vol. 13, 29–40, 2010.
10. Vazquez, C., G. Hotopan, S. Ver Hoeye, M. Fernandez, L. F. Herran, and F. Las-Heras, "Defected ground structure for coupling reduction between probe fed microstrip antenna elements," *PIERS Proceedings*, 640–644, Cambridge, USA, Jul. 5–8, 2010.

11. Abdel-Rahaman, A. B., "Coupling reduction of antenna array elements using small interdigital capacitor loaded slots," *Progress In Electromagnetics Research C*, Vol. 27, 15–26, 2012.
12. Biswas, S. and D. Guha, "Stop-band characterization of an isolated DGS for reducing mutual coupling between adjacent antenna elements and experimental verification for dielectric resonator antenna array," *Int. J. Electron. Commun. (AEÜ)*, 2012.
13. Guha, D., "Resonant frequency of circular microstrip antennas with and without air gaps," *IEEE Trans. Antennas and Propag.*, Vol. 49, No. 1, 55–59, 2001.
14. High Frequency Structure Simulator (HFSS), *Ansoft*, v 11.1.
15. Ahn, D., J. S. Park, C. S. Kim, J. Kim, Y. Qian, and T. Itoh, "A design of the low-pass filter using the novel microstrip defected ground structure," *IEEE Trans. Microwave Theory Tech.*, Vol. 49, No. 1, 86–93, Jan. 2001.
16. Chang, I. and B. Lee, "Design of defected ground structures for harmonic control of active microstrip antenna," *IEEE Antennas and Propagation Society International Symposium*, Vol. 2, 852–855, 2002.
17. Hong, J. S. and M. J. Lancaster, *Microstrip Filters for RF/Microwave Applications*, John Wiley & Sons, Inc., 2001.
18. Gupta, K. C., R. Garg, I. Bhal, and P. Bhartia, *Microstrip Lines and Slotlines*, Artech House, UK, 1996.
19. Ansoft Designer, *Ansoft*, v 2.0.